Graphene: relativistic physics in 2D

Alina Veligura
Top Master in Nanoscience

Supervisor:
Dr. Maxim Mostovoy

11 June 2007

Abstract

The discovery of graphene produces a lot of excitement in the scientific world. Isolated only 3 years ago, graphene – the two-dimensional (2D) sheet of graphite, has already become one of the most promising material for the replacement of the silicon in the nanoelectronics [1].

The purpose of this work is to review the current state of experimental research and theoretical descriptions of graphene. The review is aimed at people, who are not familiar with the subject and who want to get a general idea about it. The concepts of quantum electrodynamics, required for the explanation of the nature of charge carriers in graphene, are presented in a simple and explicit way.

The electronic structure of graphene can be obtained from nearest-neighbor, tight-binding model on honeycomb lattice. This model gives the Dirac-like spectrum of quasiparticles (electrons and holes) presented in the material. The relation between the tight-binding model and Dirac equation was discussed. We also discuss characteristic effects of QED, such as the Klein paradox and Zitterbewegung, which were never observed in particle physics. On the other hand, the experiments on these effects may be easily done by the using of graphene. We outline the problem of minimal conductivity in graphene, $\sigma_{\min} = e^2/(\pi\hbar)$ (per carrier type). The role of Zitterbewegung, as a source of "intrinsic" disorder, which gives rise to minimal conductivity of an ideal crystal; as well as disagreements with the experimental value, $\sigma_{\min} = e^2/h$, are discussed.

Contents

Introduction

According to the Nature Material statistics, the interest in graphene has grown exponentially, and the number of publications per year doubled in 2006, to a total of almost 350 papers [2].

Graphene, as a single planar sheet of sp^2-bonded carbon atoms, which are tightly packed in a honeycomb crystal lattice, theoretically was described already 60 years ago [3]. Since that time graphene band structure calculations became a "toy" problem for the students' exercises. These calculations have been also widely used for describing the properties of various carbon-based materials [4]. The theoretical discussions of 2D crystals date back to 1940's, when Landau and Peierls argued that 2D crystals do not exist. Therefore, no one believed that one could create a stable 2D sheet of atoms. However, in 2004, K. Novoselov *et al.* obtained the 2D sheet of the carbon atoms [5].

In contrast to other attempts to get a graphene sheet, this group used a top-down approach by starting with large three-dimensional crystal. The technique for the extracting of atomic monolayers is called micromechanical cleavage. Now this technique is widely used and provides high-quality graphene crystallites up to 100 μm in size, which is sufficient for most research purposes. However, while described approach suits to all research needs, other techniques that provide a high yield of graphene are required for industrial production. Among them are epitaxial growth of graphene and Si sublimation from SiC substrates. But the quality of sample obtained by these methods is not enough yet sufficient for the industrial purposes.

Graphene's unique properties arise from the collective behavior of electrons. The interaction between electrons and the honeycomb lattice causes electrons to behave as if they have absolutely no mass. Because of this, electrons in graphene are governed by the Dirac equation describing relativistic fermions (possessing spin of s = ½). Moreover these massless quasiparticles behave as though the speed of light is just 10^6 m/s, which is 300 smaller than its value in vacuum. Therefore graphene could allow one to see strange relativistic effects that have never been observed before.

For example, in QED, the Zitterbewegung – the oscillatory motion of relativistic particle, originates from the interference between particle and antiparticle states. Normally this motion is too fast to be observed. Since the Compton wavelength of Dirac fermions in graphene is of the order of one nanometer, it may be possible to spot the oscillations using a high-resolution microscope. Another as-yet unobserved QED effect is the "Klein paradox", whereby a very large potential barrier becomes completely transparent to relativistic electrons. The effect requires high enough barrier that can only be found close to a superheavy nucleus ($Z > 137$) or, even more exotically, a black hole. But recently the experiment on electron tunneling in graphene, in which the Klein effect could be displayed more easily, was offered.

Next important observation is that graphene's conductivity does not disappear even when concentration of charge carriers approaches zero. Instead, it exhibits values close to the quantum conductivity, e^2/h. For all other known materials, such a low conductivity unavoidably leads to a metal-insulator transition at low temperature, however no sign of the transition has been observed in graphene. Equally surprising is the constant disagreement between experimental, $\sigma_{\min} = e^2 / h$, and theoretical, $\sigma_{\min} = e^2/\pi h$, values of this minimal conductivity.

1. Theoretical descriptions

Because of the symmetry of the honeycomb lattice, the electrons in graphene effectively obey the relativistic Dirac equation. However, the "speed of light" that is usually found in this equation is replaced by the Fermi velocity of the electrons, which is about ~10^6 m/s. As a consequence, the solution of the Dirac equation gives a linear dispersion relation for the fermions. From this point of view, the fermions could be considered as massless particles inside the graphene.

Next chapters briefly presents the calculations of the electronic energy bands of graphene using tight-binding approximation which is usual for the theory of solids. We also showed that tight-binding model gives Dirac-like spectrum of the quasiparticles in graphene.

1.1. Tight-binding model

For long time graphene was an "elusive" 2D form of carbon. Ironically it was one of the best theoretically studied carbon allotrope. Graphene model is a starting point for study of all carbon-based systems: graphite, fullerenes, carbon nanotubes.

We will be talking about the tight-binding model in a sense where three electrons of carbon atom, which take part in σ-bonds, are tightly bonded to the atom, while the forth electron creates rather weak π-bonds with its neighbors, giving rise to two π-energy bands called bonding and anti-bonding π-bands in the Brillouin zone. The first tight-binding description of graphene was given by Wallace in 1947 [3]. He considered nearest- and next nearest- neighbor interaction for the graphene p_z orbitals, but neglected the overlap between wave functions centered at different atoms (Fig.1.1).

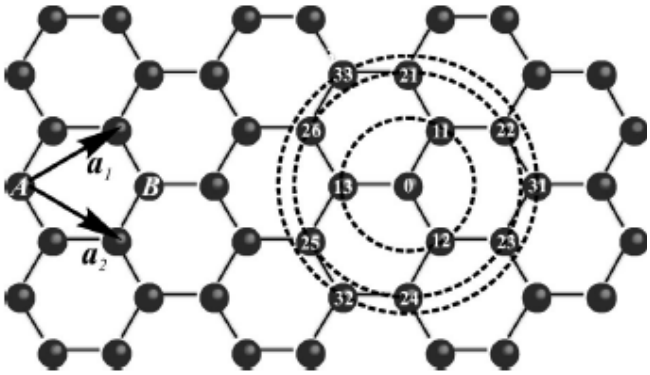

Fig.1.1
Graphene hexagonal lattice. $\boldsymbol{a}_1$ and $\boldsymbol{a}_2$ are the unit-cell vectors of graphene with a lattice constant a=2.461 Å. The unit cell contains two carbon atoms A and B belonging to the two sublattices. An atom A_0 has three nearest neighbors B_{1i}, six nextnearest neighbors A_{2i} , and three second-nearest neighbors B_{3i} [6].

The other, nowadays better known, tight-binding approximation was nicely described by Saito *et al.* [4]. It considers an overlap between the basis functions, but includes only interactions between nearest neighbors within the graphene sheet. The nearest-neighbor Hamiltonian does not accurately reproduce the π and π* graphene bands over a sufficiently large range of the Brillouin zone. If up to third-nearest neighbors are included, the tight-binding approximation quite accurately describes first-principles results over the entire Brillouin zone [6].

But independent on the approximations made the most important results in the intersection points of the valence and conduction bands are remained similar. Let's present brief description of the tight-binding model for the honeycomb structure and emphasize on some important moments.

In Fig.1.2 we show the unit cell and the Brillouin zone of graphene, where $\vec{a}_1$ and $\vec{a}_2$ are unit vectors in real space, and $\vec{b}_1$ and $\vec{b}_2$ are reciprocal lattice vectors. In the *x,y* the real and reciprocal lattice vectors will be expressed as

Lattice vectors:

$$\vec{a}_1 = a\left(\frac{\sqrt{3}}{2}, -\frac{1}{2}\right)$$

$$\vec{a}_2 = a(0,1)$$

Reciprocal lattice vectors:

$$\vec{b}_1 = \frac{4\pi}{\sqrt{3}a}(1,0)$$

$$\vec{b}_2 = \frac{4\pi}{\sqrt{3}a}\left(\frac{1}{2}, \frac{\sqrt{3}}{2}\right)$$

Vectors connect three nearest neighbors:

$$\vec{f}_1 = \frac{a}{\sqrt{3}}(1,0)$$

$$\vec{f}_2 = \frac{a}{\sqrt{3}}\left(-\frac{1}{2}, -\frac{\sqrt{3}}{2}\right)$$

$$\vec{f}_3 = \frac{a}{\sqrt{3}}\left(-\frac{1}{2}, \frac{\sqrt{3}}{2}\right)$$

The unit cell of the hexagon lattice contains two atoms A and B, they are not equivalent between each other, because there is no reciprocal vector in the reciprocal space which may connect these two points. Thus, the honeycomb structure could be present as a superposition of two sublattices: containing either A or B atoms.

Fig.1.2
The unit cell (A) and reciprocal vectors of graphene.

The translation vector of sublattices A and B are $\vec{x}_n = n_1\vec{a}_1 + n_2\vec{a}_2$ and $\vec{x}_{n+f_a} = \vec{x}_n + \vec{f}_a$, correspondingly. The Hamiltonian of the tight-binding model has the form

$$H = t\sum_{n,a,\sigma}(b^+_{n+f_a,\sigma}a_{n,\sigma} + a^+_{n,\sigma}b_{n+f_a,\sigma}), \qquad (1)$$

where $a_{n,\sigma}, b_{n+f_a,\sigma}$ are annihilation operators of the electrons on the corresponding sites of A and B sublattices. As one can see from Eq.(1) the Hamiltonian has the particle-hole symmetry on honeycomb lattice: it remains invariant upon substitution of

$a_{n,\sigma} \to a^+_{n,\sigma}$ and $b_{n+f_a,\sigma} \to -b^+_{n+f_a,\sigma}$. This means that for every electron state with energy ε the equation also describes the presence of the state with energy equals to - ε. Therefore, in contrast to condensed matter physicis where electrons and holes are normally described by separate Schrödinger equations which involve different masses for the particles, the electron and hole states in graphene are interconnected [7]. The "Particle-hole symmetry" in graphene is analog of charge-conjugation symmetry in quantum electrodynamics (QED).

Going to the momentum space the Eq.(1) has next form

$$H = t\sum_q \left[\xi_{\vec{q}} a^+_{\vec{q}} b_{\vec{q}} + \xi^*_{\vec{q}} b^+_{\vec{q}} a_{\vec{q}}\right], \qquad (2) \qquad \text{where } \xi_{\vec{q}} = \sum_{a=1}^{3} e^{i\vec{q}f_a};$$

$$a_n = \frac{1}{\sqrt{N}}\sum_q e^{i\vec{q}\vec{x}_n} a_{\vec{q}}; \qquad b_{n+f_a} = \frac{1}{\sqrt{N}}\sum_q e^{i\vec{q}(\vec{x}_n+\vec{f}_a)} b_{\vec{q}};$$

Here we took in account only three nearest neighbors, which doesn't influence the result of the calculations near the Dirac point: the edge of the Brillouin zone, where $\xi_{\pm\vec{q}} = 0$, $\vec{q} = \vec{q}_1 + \vec{k}$, $ka << 1$ in case of small deviations the function behaves linearly $\xi_{\vec{q}} \cong e^{i\frac{2\pi}{3}} \approx e^{-i\frac{\pi}{3}} \frac{\sqrt{3}a}{2}(k_x - ik_y)$, $\xi_{-\vec{q}_1+\vec{k}} = \xi^*_{\vec{q}_1-\vec{k}}$

substitution into Eq.(2) gives

$$H \approx \hbar v_f (a^+_{\vec{q}_1+\vec{k}_1} b^+_{\vec{q}_1+\vec{k}_1}) \begin{pmatrix} 0 & e^{i\frac{\pi}{3}}(k_x - ik_y) \\ e^{-i\frac{\pi}{3}}(k_x + ik_y) & 0 \end{pmatrix} \begin{pmatrix} a_{\vec{q}_1+\vec{k}_1} \\ b_{\vec{q}_1+\vec{k}_1} \end{pmatrix}.$$

Using Pauli matrices, $\vec{\sigma} = /\sigma_x, \sigma_y/$, σ_z, notations one may show

$$H = v_f \sum_{i=1,2} \psi^+_i \vec{p}\vec{\sigma}\psi_i, \qquad (4)$$

where $\hbar v_f = \frac{\sqrt{3}at}{2}$;

$$\begin{pmatrix} a_{\vec{q}_1+\vec{k}_1} \\ b_{\vec{q}_1+\vec{k}_1} \end{pmatrix} = e^{i\frac{\pi}{6}\sigma_z}\psi_1, \quad \begin{pmatrix} a_{-\vec{q}_1+\vec{k}_1} \\ b_{-\vec{q}_1+\vec{k}_1} \end{pmatrix} = e^{-i\frac{\pi}{6}\sigma_z}\sigma_y\psi_2. \qquad (5)$$

Eq.(4) shows one of the most important properties of graphene's quasiparticles. They have a linear energy dispersion in the area of Dirac points. At first this equation for

graphene was confirmed experimentally by Geim *et al.* [8], Eq.(5) actually represent mentioned quasiparticles, described by two-component wave functions (ψ_1, ψ_2) which are needed to define the relative contributions of the A and B sublattices in the quasiparticles' make-up [9]. This two-component description for graphene is very similar to the spinor wave function in QED, but here "spin" index indicates the subblattice rather then real spin of the electrons and is usually named "pseudospin" σ [10,11]. This allows one to introduce chirality – formally a projection of pseudospin on the direction of motion – which is positive and negative for electrons and hole, respectively.

The linear energy dispersion in the vicinity of Dirac points, and the zero-energy gap in these points, are presumably consequences of the symmetry of the lattice and are independed on the approximations considered [3,6]. The solution of Eq.(2) in the whole region of Brillouin zone gives cosine like eigenvalues of energy [3,4,10,11].

$$E_{g2D}(k_x, k_y) = \pm t\left\{1 + 4\cos(\frac{\sqrt{3}k_x a}{2})\cos\frac{k_y a}{2} + 4\cos^2(\frac{k_y a}{2})\right\}^{1/2}$$

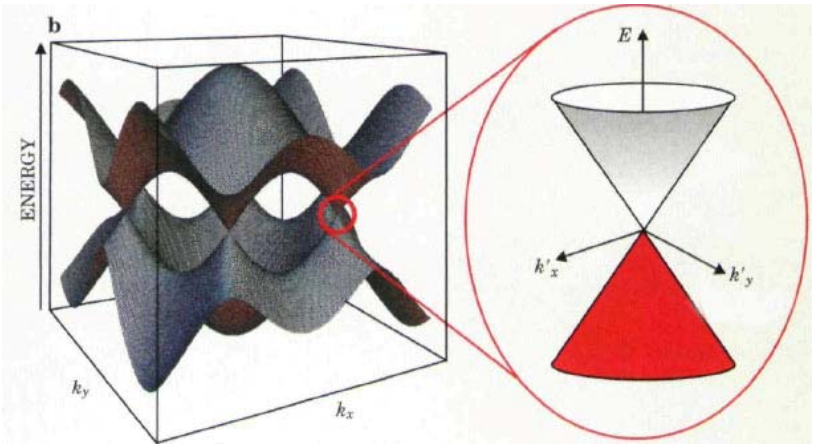

Fig.1.3
A band-structure picture of graphene with conical spectrum of fermions in the vicinity of Dirac points [12].

As one may see in Fig.1.3 the upper half of the energy dispersion curves describes the π^*- energy anti-bonding band (conductive band), and the lower half is the π-energy bonding band (valence band). The conduction and valence bands overlap at the Dirac points through which the Fermi energy passes. The existence of the zero-gap comes from the symmetry requirement that the two carbon sites A and B in the hexagonal lattice are equivalent to each other [4]. Thus fermions have the conical spectrum inside graphene, where an electron with energy ε propagating in the positive dirraction originates from the same branch of the spectrum as the hole with energy $-\varepsilon$ propagating in the opposite direction. At zero temperature the valence zone is completely filled, and the conduction band is completely empty. At nonzero temperature the Fermi surface will be smeared in amount comparable to kT.

1.2. Dirac equation. Massless fermions

Amount of the literature devoted to graphene mostly either takes as a statement relativistic nature of the electrons inside the graphene [2,8-10] or gives QED based derivations which are rather unclear to those who are not familiar with this part of theoretical physics [11,13-14]. Therefore here I would like to present quite simple but important logical steps which connects tight-binding model results with Dirac Hamiltonian.

Classical Dirac Hamiltonian is given by

$$H = \vec{\alpha} c\vec{p} + \beta mc^2 \qquad (6)$$

where the Hermitian, dimensionless matrices $\vec{\alpha}$ and β are to be determined and $\vec{p}$ denotes the three-dimensional momentum vector [15].

The requirements to α, β are next:

$\beta^2 = 1;$ $\beta\alpha_i + \alpha_i\beta = 0;$ $\alpha^2 = 1;$ $\alpha_j\alpha_i + \alpha_i\alpha_j = 2\delta_{i,j}$ *(i=x,y,z).*

In the two dimensional case the Dirac matrices can be identified with the Pauli matrices:

$\alpha_1 = \sigma_x;\ \alpha_2 = \sigma_x;\ \beta = \sigma_z$ then (4) will be given

$$H = v_f \sum_{i=1,2} \psi_i^+ \vec{p}\vec{\alpha}\psi_i \qquad (7)$$

Let's show that Dirac Hamiltonian shows the same results for massless particles.

Putting (6) in square

$$H^2 = \left[c\vec{\alpha}\vec{p} + \beta mc^2\right]^2 = m^2c^4\beta^2 + c^2 p_i p_j \alpha_i\alpha_j + mc^3 p_i(\beta\alpha_i + \alpha_i\beta)$$

and applying properties of Pauli matrices one obtains

$H^2 = m^2c^4 + c^2\vec{p}^2$, then $\varepsilon_{\vec{p}} = \pm\sqrt{m^2c^4 + c^2\vec{p}^2}$

for massless particle $m = 0$ and if to count from the Fermi level $c \to v_f$

$$\varepsilon_{\vec{p}} = \pm v_f \vec{p}$$ compare with (7).

All massless particles have the same energy dispersion as photons. Therefore, quasiparticles in graphene are massless particles described by the equation (7) or (4).

In these chapters we showed that charge carriers in graphene mimic ultrarelativistic particles and may be described by the Dirac equation which is typical for QED. The tight-binding model, by which the system is described, gives an intersection of valence and conduction bands of the materials in the vicinity of Brillouin zone edges. The existence of the zero-gap comes from the symmetry requirements of the honeycomb lattice. As the fermion spectrum near intersection points is conical, they behave like massless particles obeying charge-conjugation symmetry.

2. Unobservable QED effects.

The graphene discovery offered a possibility of testing various QED effects, among which the "gedanken" Klein paradox and "Zitterbewegung" stand out because these effects are unobservable in particle physics.

The Klein paradox is the perfect tunneling of relativistic fermions through arbitrary high and wide barriers [16]. The experiment is conceptually easy to implement in graphene [17]. There are not so many papers on this subject, but the suggested experiments [17,18] look very promising (taking in account that the discovery of graphene was made only 3 years ago). Especially interesting observation was made by Cheianov *et al*. in Ref.[19], where they showed that doped graphene can serve as a negative refraction medium.

These papers show the efforts to find experimentally accessible analogues with which one can study otherwise inaccessible relativistic and quantum electrodynamics effects. For example, the Klein paradox predicts the phenomenon of pair production in vicinity of arbitrary high and wide barriers [16], which is a kind of bizarre behavior that would normally require, in cosmological terms, superheavy atoms or black holes. Thus possible observation of Klein paradox in graphene gives a tabletop experiment to study cosmological objects [20] and to answer some theoretically predicted effects like Hawking radiation emitted from beyond the event horizon of black holes.

2.1 Klien paradox in classical QED

In 1929 Oskar Klein proposed a thought experiment to explore the paradoxical implications of the Dirac equation, which had been formulated just the year before by Paul Dirac to provide a description of mechanics and special relativity [17]. The essence of the experiment lies in the prediction that according to the Dirac equation, fermions can pass through strong repulsive potentials without the exponential damping expected for a quantum tunneling process. Here we omit of the scattering problem for Dirac equation and only present Klein's results.

Consider an electron of energy E, mass m and momentum k reflecting off the potential step (see Fig.2.1):m

$V(x) = V,\ x > 0;\ V(x) = 0,\ x < 0.$

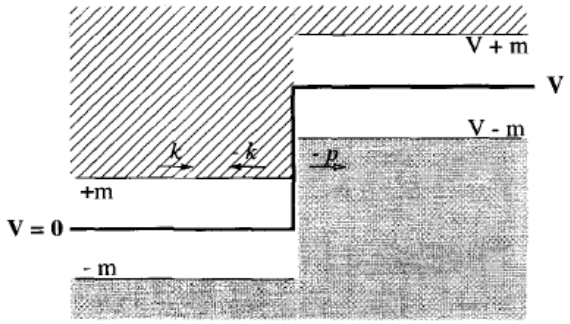

Fig.2.1.

An electron of energy E scattering off a Klein step of height $V > 2mc^2$. The electrons are shown with solid arrowheads; the hole state has a hollow arrowhead. [16].

The reflection and transmission coefficients for the incoming electron R_s, T_s, if V is "large" ($V > 2mc^2$), are given by

$$R_s = \left(\frac{1-\kappa}{1+\kappa}\right)^2, \qquad T_s = \frac{4\kappa}{(1+\kappa)^2}, \tag{8}$$

where κ is the kinematic factor: $\kappa = \left[\frac{(V-E+m)(E+m)}{(V-E-m)(E-m)}\right]^{1/2}$ (9)

Let $V \to \infty$ for fixed E. Then from Eq.(9) κ tends to a finite limit and hence T_s tends to a non-zero limit: there is non-zero probability for the particle to penetrate inside the step.

The explanation of the paradox is schematically given in Fig. 2.1. When the high of Klein step is $V > 2mc^2$, the particle continuum (slanted background) and the hole continuum (shadowed background) overlap. This means that sufficiently strong potential, being repulsive for electrons, is attractive for positrons allowing for positron (hole) state inside the barrier, which align in energy with the electron continuum outside. Matching between electron and positron wavefunctions across the barrier leads to the high-probability tunneling described by the Klein paradox. Thus, the condition for perfect tunneling is having an incident particle of energy within the overlap zone of particle/hole continuums: $mc^2 < E < V - mc^2$. The essential feature of QED responsible for the effect is the fact that states with positive and negative energies (electrons and holes) are intimately related, being described by different components of the same spinor wavefunction − charge-conjugation symmetry (as was discussed in Ch.1.1).

Similarly, one can solve the problem for a square barrier. I would not present these results (partly they will be treated in next paragraph). Here I only discuss an analogy between electromagnetic wave propagation and the scattering of Dirac particles.

The square barrier for the particle with momentum p is

$$V(x) = V,\ |x| < a;\ V(x) = 0,\ |x| > a.$$

In this case the reflection and transmission coefficients are given by

$$R = \frac{(1-\kappa^2)\sin^2(2pa)}{4\kappa^2 + (1-\kappa^2)\sin^2(2pa)},\ T = \frac{4\kappa^2}{4\kappa^2 + (1-\kappa^2)\sin^2(2pa)}.$$

From these equations we find that for $2pa = N\pi$ the electron passes right through the barrier with no reflection − transmission resonance occurs.

From Eq.(8) one may see that T_s and R_s correspond to reflection and transmission coefficients in transparent media with differing refractive indices: thus k is nothing more than effective fermionic refractive index resulting from the change of particle's velocity in the presence or absence of potential. From this point of view, tuning the momentum p to obtain a transmission resonance for scattering off a square barrier is nothing more than finding a frequency for which a given slab of refractive material is transparent. "A potential hill of sufficient height acts as Fabry-Perot etalon for electrons, being completely transparent for some wavelengths, partly or completely reflecting for others" [21].

Owing to the extreme conditions involved − the potential step of twice the rest energy of an electron ($V > 2mc^2$) would require an electric field of more than 10^{16} V·cm^{-1}− it is only expected to occur under extreme circumstances: superheavy atoms (where nuclear charge Z>137) or event horizon of black holes.

2.2 Klein paradox in graphene

Because quasiparticles in graphene accurately mimic Dirac fermions, this condensed matter system makes it possible to set up a tunneling experiment similar to that analyzed by Klein. Katsnelson *et al*. in their paper [18] considered the rectangular shaped potential barrier (Fig.2.2):

$$V(x) = \begin{cases} V_0, & 0 < x < D \\ 0, & otherwise \end{cases}.$$

Such barrier may be created using the electrical field effect [1,5] or by local chemical doping. An important advantage of using graphene is that electrons are massless and, therefore, formally there is no theoretical requirement for minimal electrical field $\mathcal{E}$ to form hole states under the barrier (to achieve the overlap of electron and hole continuums). To create a well-defined barrier in realistic graphene samples with a disorder, fields $\mathcal{E} \approx 10^5$ V·cm^{-1} routinely used in experiments should be sufficient [5], which is eleven orders of magnitude lower than the necessary for the observation of the Klein paradox for elementary particles.

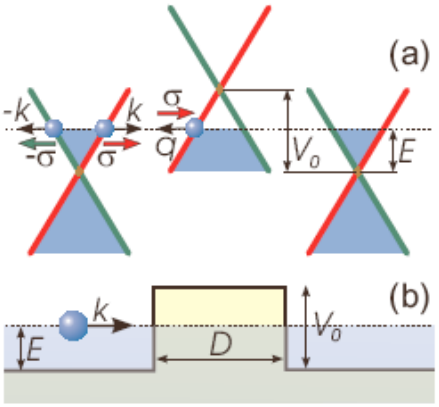

Fig.2.2
Tunneling through a potential barrier in graphene.
(a) Schematic diagrams of the spectrum of quasiparticles in graphene.
(b) The three diagrams illustrate schematically the positions of the Fermi energy E across the potential barrier of high V_0 and width D [18].

The authors of Ref. [18] assumed that the incident electron propagates at an angle ϕ with respect to the x axis. The following expression for the reflection coefficient r was found:

$$r = 2ie^{i\phi}\sin(q_x D)\frac{\sin\phi - ss'\sin\theta}{ss'[e^{-iq_x D}\cos(\phi+\theta) + e^{iq_x D}\cos(\phi-\theta)] - 2i\sin(q_x D)},$$

where $q_x = \sqrt{(E-V_0)^2/\hbar^2 v_f^2 - k_y^2}$ and $\theta = \tan^{-1}(k_y/q_x)$ is the refraction angle; $s = signE$, $s' = sign(E-V_0)$.

Transmission probability of the electron could be find as $T = |t|^2 = 1 - |r|^2$. In the limit of high barriers $|V_0| >> |E|$ the expression for T can be simplified to

$$T = \frac{\cos^2\phi}{1 - \cos^2(q_x D)\sin^2\phi} \qquad (10).$$

From the Eq.(10) it follows that there are resonance conditions $q_x D = \pi N$, $N = 0, \pm 1, \ldots$ under which the barrier becomes transparent (T = 1). More significantly, the barrier remains always perfectly transparent for angles close to the normal incidence ϕ = 0 (Fig.2.3).

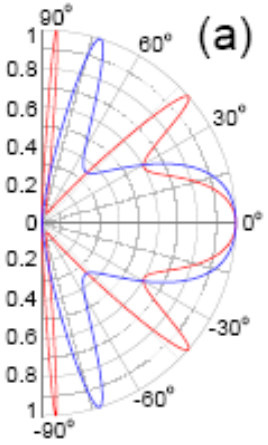

Fig.2.3
Klein-like quantum tunneling in graphene.
Transmission probability T through a 100 nm wide barrier. The barrier heights V_o are 200 meV (red curve) and 285 meV (blue curve) [18].

The angular dependence of transmission probability T in Fig.2.3 was calculated for electron concentration $n = 0.5\times10^{12}$ cm^{-2} outside the barrier. Inside the barrier, hole concentrations p are 1×10^{12} and 3×10^{12} cm^{-2} for red and blue curves, respectively (such concentrations are most typical in experiments with graphene).

This perfect tunneling may be explained in terms of the pseudospin conservation. Indeed, in the absence of pseudospin-flip process, an electron moving to the right can be scattered only to the right moving electron state or left moving hole state. Illustration of this is given in Fig.2.2a, where charge carriers from the "red" branch of the band diagram can be scattered into states within the same "red" branch but can not be transformed into any state on the "green" branch. The latter scattering event would require the pseudospin to be flipped. The matching between directions of pseudospin σ for quasiparticles inside and outside the barrier results in perfect tunneling.

2.3. Implications for experiment

Let me briefly present an idea of experimentally testing the Klein paradox and related phenomena using graphene device [18].

On possible experimental setup is shown in Fig.2.4.

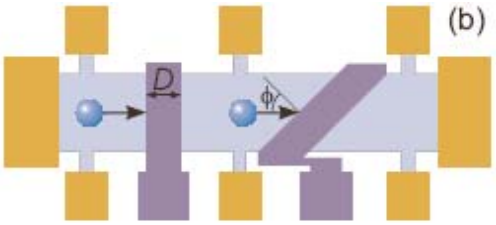

Fig.2.4
Schematic diagram of tunneling experiment in graphene.
Blue elements −graphene;
Dark-blue − local gates;
Orange − potential contacts [16].

Graphene (blue) has two local gates (dark-blue) that create potential barriers of variable height. Intrinsic concentrations of charge carriers are usually low (~ 10^{11} cm^{-2}),

whereas concentration up to 1×10^{13} cm^{-2} can be induced under gated regions by the electrical field effect [5]. This allows potential barrier with height up to $V_0 \approx 0.4$ eV. The voltage drop across the barriers is measured by using potential contacts shown in orange. One may analyze the voltage drop as a function of applied gate voltage, which reflects transparency for different V_0. Results in Fig.2.3 shows that resistances should exhibit different dependence on V_0 for two 90°- and 45°- barriers. The 90°-barrier has to have low resistance and no significant changes in it with changing gate voltage. In comparison, the 45°-barrier is expected to have much higher resistance and show a number of tunneling resonances as a function of gate voltage.

2.4. Charge carriers confinement in graphene

As consequence of Klein paradox all potential barriers are relatively transparent ($T \approx 1$ at least for some angles) for quasiparticles in graphene. This does not allow charge carriers to be confined by potential barriers that are smooth on atomic scale. Therefore, different electron and hole "puddles" induced by disorder are not isolated but effectively percolate, thereby suppressing localization. As a result of this, the conducting channels in graphene can not be pinched off, which limits possible application of graphene-based field effect transistors in logical electronics.

However, Martino *et al.*, in their paper [22] described a completely different and hitherto unnoticed way of confining Dirac quasiparticles in graphene by magnetic barriers. Employing existing technology, the required inhomogeneous static magnetic field configurations can be created using ferromagnetic layers located beneath the substrate on which the graphene layer is deposited.

To find the transmission probability of the electrons for magnetic barrier, one needs to solve time-independent Dirac equation for the spinor $\psi(x,y)=(\psi_1, \psi_2)$ (Eq.(5)) at energy $E = v_f \varepsilon$ in the presence of slowly varying magnetic field $\boldsymbol{B}$ = curl$\boldsymbol{A}$:

$$\vec{\sigma}\left[\mathbf{p} + \frac{e}{c}\mathbf{A}(x,y)\right]\psi(x,y) = \varepsilon\psi(x,y)$$

(for comparison see Eq.(4)).

Let me present the solution of the equation for a square-well magnetic barrier, where $B = B_0\hat{e}_z$ within the strip $-d \le x \le d$, but $B = 0$ otherwise: $B(x,y) = B_0\theta(d^2 - x^2)$ with the Heaviside step function θ. The magnetic field is oriented perpendicular to the graphene xy plane.

Again omitting the derivation, the dependence of the emergence angle ϕ' at the right barrier on the kinematic incidence angle ϕ is given by

$$\sin\phi' = \frac{2d}{\varepsilon l_B^2} + \sin\phi,$$

where $l_B = \sqrt{c/eB_0}$ is the magnetic length.

This equation implies that for certain incidence angles ϕ, no transmission is possible. In fact, under the condition $\varepsilon l_B \le d / l_B$ every incoming state is reflected, regardless on the incidence angle. In essence, all states with cyclotron radius (defined under the magnetic barrier) less then d will bend and exit backwards again (Fig.2.5).

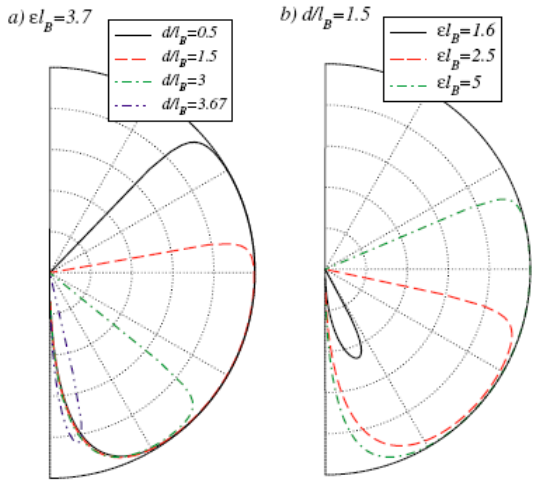

Fig.2.5
The transmission probability $T(\phi)$ for magnetic barrier of width $2d$ at various energies ε. The outermost semicircle corresponds to $T = 1$, the center $T = 0$, with grid spacing.
(a) T as a function of barrier width for fixed energy, $\varepsilon l_B = 3.7$.
(b) Same as a function of ε for $d / l_B = 1.5$ [22].

In Fig.2.5 the transmission probability T is zero for $d / l_B \geq 3.7$ and fixed energy $\varepsilon l_B = 3.7$.

Thus, the main finding of the paper is that in contrast to electrostatic barriers, magnetic barriers are able to confine Dirac quasiparticles.

In summary, the effect of the Klein-like tunneling − unimpeded penetration of relativistic particles through extreme (high and wide) potential barriers − is well understood, so there is no longer paradox. But physicists thought that the effect can only be observed under extreme conditions, e.g. in superheavy atoms or in the gravitational tide at the edges of black holes. The presence of relativistic massless quasiparticles in graphene opens the possibility to test the Klein paradox in laboratory conditions using relatively small (and routinely accessible in experiments) barriers (less then 1 eV). Due to the zero band gap in graphene, there are always hole states aligned in energy and available inside the barrier (in the valence band) for the incoming electron. The local potential barrier just inverts the sign of charge carriers underneath it, creating holes playing the role of positrons or vise versa. The suggested tunneling experiment in graphene [18] makes possible to study the angle and voltage gate dependence of transmission probability of electrons through the barrier. From another point of view, the Klein-like tunneling in graphene results in the charge carrier delocalization in the material, which potentially limits graphene application in quantum dots, quantum point contacts and logical elements. The novel way of confining of Dirac quasiparticles by magnetic barriers was suggested in Ref. [22].

2.5. Zitterbewegung effect

The Dirac equation has had an incredible success rate when its predictions are correctly interpreted. Its negative energy solution leads to the prediction of antiparticles. In 1930 Erwin Schrödinger proposed the existence of Zitterbewegung motion as a result of his analysis of the wave packet solutions of the Dirac equation for relativistic electrons in free space.

Zitterbewegung ("jitter") is a theoretical helical or circular motion of elementary particles, in particular electrons, caused by an interference between positive and negative energy states. This interference produces what appears to be a fluctuation (at the speed of light) of the position of an electron around the median, with a circular frequency of $2m_e c^2/\hbar$, or approximately 1.6×10^{21} Hz. Exactly Zitterbewegung motion is responsible for producing of particle spin and magnetic moment. The effect is also connected to the proven existence of the Darwin term in atomic physics [23].

"Jittery" motion arises because it is not possible to localize the wavefunction of a relativistic particle in a distance smaller than its Compton wavelength. An electron moving at relativistic speeds can spawn its own antiparticle, and the interaction between the two causes the path of the electron to jitter. Normally this motion occurs too rapidly to be observed. In a solid however, the equivalent of an antiparticle is hole (as was described in Sec.1). Thus, when Dirac fermions are confined in graphene sample, zitterbewegung can be interpreted in terms of mixing of electron and hole state. Since the Compton wavelength of the Dirac fermions in graphene is of the order of a nanometer, it may be possible to spot the jitter using a high-resolution microscope [24].

Let me start with Eq.(4). According to it, the expression for the current operator is

$$\vec{j} = ev_F \sum_P \psi_p^+ \vec{\sigma} \psi_P ,$$

where the spin and valley indices are omitted.

Straightforward calculations [11] give for the time evolution of the electron operators $\psi_P(t) = \frac{1}{2}\left[e^{-i\omega_P t}(1+\frac{\vec{p}\vec{\sigma}}{p}) + e^{i\omega_P t}(1-\frac{\vec{p}\vec{\sigma}}{p}) \right]\psi_P$; while for the current operator we obtain

$$\vec{j} = \vec{j}_0(t) + \vec{j}_1(t) + \vec{j}_1^+(t);$$

$$\vec{j}_0(t) = ev_F \sum_P \psi_p^+ \frac{\vec{p}(\vec{p}\sigma)}{p^2}\psi_P ,$$

$$\vec{j}_1(t) = \frac{ev_F}{2}\sum_P \psi_p^+ \left[\vec{\sigma} - \frac{\vec{p}(\vec{p}\vec{\sigma})}{p^2} + \frac{i}{p}\vec{\sigma}\times\vec{p} \right]\psi_P e^{2i\omega_P t}, \quad (11)$$

where $\omega_P = vp/\hbar$ is the particle frequency. The last term in Eq.(11) corresponds to the Zitterbewegung: the electrical conduction through an ideal graphene strip is associated with time-dependent current fluctuations.

In condensed matter physics, the Zitterbewegung presents nothing but a special kind of inter-band transitions with creation of virtual electron-hole pairs. These could be shown from the Eq.(11) after unitary transformation, generated by the operator $U_P = 1/\sqrt{2}(1+im_P\sigma)$, where $m_p = (\cos\phi_p, -\sin\phi_P)$ and ϕ_P is the polar angle of the

vector P. The transformation diagonalizes the Hamiltonian. Then the oscillating term in equation (11) corresponds to the inter-band transitions:

$$U_P^+ j_P^x U_P = ev_F \begin{pmatrix} -\cos\phi_P & -i\sin\phi_P e^{-i\phi_P+2i\omega_P t} \\ i\sin\phi_P e^{i\phi_P-2i\omega_P t} & \cos\phi_P \end{pmatrix}.$$

It is the Zitterbewegung, i.e. the oscillating term $j_1(t)$ which is responsible for nontrivial behavior of the conductivity for zero temperature and zero chemical potential. In other words, it plays a role of "intrinsic" disorder in the system which causes non-zero minimal conductivity of an ideal (without defects) crystal.

In an interesting paper [25] the effect of Zitterbewergung in graphene, spintronic and superconducting systems is described from a general point of view. It was shown that the Zitterbewergung is not necessarily a relativistic effect, but it is related to two component nature of eigenfunctions of charge carriers. To put it differently, this phenomenon is the direct consequence of the pseudospin degree of freedom.

3. Minimal quantum conductivity

Minimum quantum conductivity has been predicted for Dirac fermions by a number of theories [11,14]. Recently it was verified experimentally [5]. The graphene conductivity, σ_{min}, doesn't disappear in the limit of vanishing charge density, n, but instead exhibits values close to the quantum conductivity, e^2/h, per carrier type [8].There are however sizable disagreements between theoretical and measured values of the conductivity [1]. Most theories suggest $\sigma_{min} = 4e^2/h\pi$ (4 is due to the degeneracy of electron states), which is about π times smaller than the typical values observed experimentally. This disagreement has become known as "the mystery of missing pie" and it still unresolved. Let us take a closer look at this problem.

3.1. Experimental observations

In Ref.[5] the electric field effect in graphene was observed at first. In Fig.3.1E one may see a schematic view of the device used by authors. To separate the graphene sheet from the "gate" material (n^+Si) the insulator layer of SiO_2 between them was placed. Thus the typical field effect transistor scheme was achieved. By applying voltage to the gate, V_g, one can induce either positive or negative charge carriers in graphene dependent on the sign of V_g.

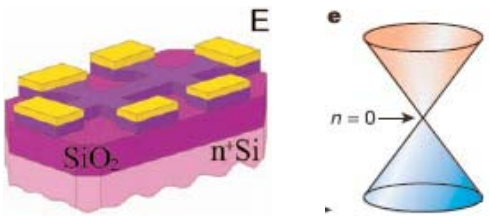

Fig.3.1.
E) Schematic view of the device used for the observation of electric field effect in graphene (dark blue). The distance between electrodes (orange) is about 1 μm[5].
e) Electronic spectrum of graphene. The point of vanishing charge carrier concentration is shown [8].

The rustles of the measurement of conductivity, σ_{min}, at zero gate voltage were quite unusual. The Dirac-like spectrum of charge carriers in graphene implies vanishing

concentration of both carriers near the Dirac point $E = 0$ (Fig.3.1e), which suggests that low-T resistivity of the zero-gap semiconductor should diverge at $V_g = 0$. However, the measurements showed that conductivity increases linearly with increasing gate voltage for both polarities and at zero-filed point reaches its minimal value $4e^2/h$ (Fig.3.2A).

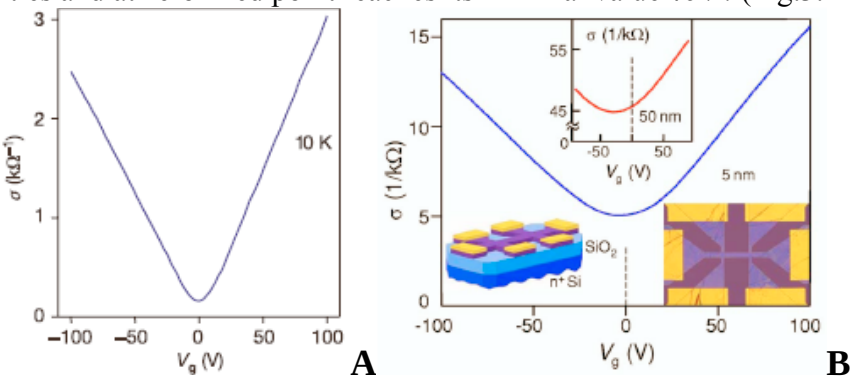

Fig.3.2.
Conductivity, σ, as a function of gate voltage, V_g:
A) clear graphene sheet [8];
B) n- doped graphite films with width $d \approx 5$ and 50 nm (main panel and upper inset, respectively) [26].

It should be noted that the discussed minimum in σ was often found to be shifted from zero V_g [5,26]. The sample-dependent shift could occur in both directions of V_g and is attributed to chemical doping of graphite surfaces during microfabrication. The shift to positive voltages is attributed to an unintentional doping of the films by absorbed water [5], while the exposure of the annealed films to NH_3 leads to the shift in direction of negative voltages determined by graphene film n-doping (Fig.3.2B) [26].

Importantly, it is resistivity (or conductivity) rather than the resistance (or conductance) that is quantized in graphene. The resistance R measured experimentally scales in the usual manner as $R = \rho L/w$ with changing length L and width w of the devices. Thus, the effect is completely different from the conductance quantization observed previously in quantum transport experiments. Actually, the conductivity minimum is an intrinsic property of electronic system described by the Dirac equation [11,14]. It results from the fact that localization effects caused by disorder in such systems are strongly suppressed. This can be qualitatively explained as follows. The mean free path l of charge carriers in a metal can never be shorter than de Broglie wavelength k_F^{-1}. Then, $\sigma = ne\mu$ can be rewritten as $\sigma = (e^2/h)k_F l$, so σ cannot be smaller than, e^2/h for each type of carrier. This argument is known to have failed for 2D systems with a parabolic spectrum, in which disorder leads to localization and eventually to insulating behavior [18]. For 2D Dirac fermions, no localization is expected [18,20,23]. Most theories suggest that a 2D gas of Dirac fermions should exhibit a minimal conductivity of about $e^2/\pi h$, which apart from numerical coefficient agrees with the experiment.

In next chapter the theoretical description of this minimal conductivity problem is presented.

3.2. Theoretical description of minimal conductivity in graphene

The first results on the theoretical combination of graphene electron transport properties and a characteristic property of Dirac chiral fermions were obtained by Katsnelson [11,18,27]. The intrinsic nature of Dirac fermions gives rise to minimal conductivity even for an ideal crystal, that is, without any scattering processes. The simplest way for the theoretical consideration is the Landauer approach [11]. Assuming that the sample is a ring of length L_y in y direction; author used the Landauer formula to calculate the conductance in the x direction (Fig. 3.3). The convenient boundary conditions are not physical, but to get finite transparency one should choose $L_x << L_y$.

In the coordinate representation the Dirac equation at zero energy takes the form

$$\begin{aligned}(K_x + iK_y)\psi_1 = 0\\ (K_x - iK_y)\psi_2 = 0\end{aligned}, \text{ where } K_i = -i\frac{\partial}{\partial x_i}.$$

The solutions of these equations are $\begin{aligned}\psi_1 = \psi_1(x+iy)\\ \psi_2 = \psi_2(x-iy)\end{aligned}$, which are complex conjugated functions which are general solutions.

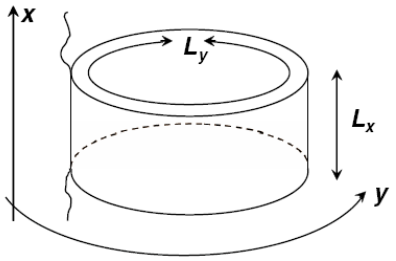

Fig.3.3.
Geometry of the sample. The direction of the current is parallel to the x axis [27].

Due to periodicity in y direction both wave functions should be proportional to $e^{ik_y y}$ where $k_y = 2\pi n/L_y$, $n = 0, \pm1, \pm2, \ldots$ This means that the dependence on the x is also fixed: the wave functions are proportional to $\exp(\pm 2\pi n x/L_y)$. The introduced boundary conditions at the sample edges are $x = 0$ and $x = L_x$. The assumption is that the sample is doped graphene with the Fermi energy $E_F = vk_F = -V_0$. The wave functions in the sample are supposed to have the same y-dependence, that is, $\psi_{1,2}(x,y) = \psi_{1,2}(x)e^{ik_y y}$. Requiring continuity of the each wave function at the edges of sample, one can find the transmission coefficient:

$$T_n = \left|t(k_y)\right| = \frac{\cos^2\phi}{\cosh^2(k_y L_x) - \sin^2\phi}, \qquad \text{where } \sin\phi = k_y / k_F;\ k_x = \sqrt{k_F^2 - k_y^2}\ .$$

Further, one should assume that $k_F L_x >> 1$ and put $\phi = 0$ in equation. Thus, the trace of the transparency which is just the conductance per valley per spin is

$$g = \frac{e^2}{h}tr(T) = \frac{e^2}{h}\sum_{n=-\infty}^{\infty}\frac{1}{\cosh^2(k_y L_x)} \cong \frac{e^2}{h}\frac{L_y}{\pi L_x}. \qquad (11)$$

The conductance then equals $\sigma\frac{L_y}{L_x}$ and the conductivity is $\frac{e^2}{\pi h}$. Experimentally, it is close to e^2/h [5,8], that is in π times larger than present estimation.

Exactly Zitterbewegung effect is responsible for the minimal conductivity observation, which is physically explains as the impossibility to localize ultrarelativistic particles and to measure their coordinates. Zitterbewegung introduces the "intrinsic" disorder (Eq.(11): oscillation part) in the system which causes presence of a minimal conductivity even for ideal (without scattering) crystals at low temperatures. The relativistic "jittering" of electron, due to the interference between positive and negative energy states, could be interpreted in terms of classical physics as an interaction of electron with some potential caused by the presence of disorder in crystal.

Following Ref.[28] one can estimate the Fano factor (ratio of noise power and mean current) in graphene. The results of that paper, where the same Landauer approach was used, imply that relativistic quantum mechanics (which describes Zitterbewegung) produces the same shot noise as classical diffusion. They predict that the noise is the largest, compared to the mean current, when the Fermi energy is adjusted (by the gate voltage, for example) such that electrons and holes are degenerate. At this Dirac point the Fano factor takes the universal value 1/3 for short and wide strips. Observation of this sub-Poissonian shot noise would be a unique demonstration of electrical noise produced by relativistic quantum dynamics.

Already in his first paper about graphene [1] Katsnelson pointed out that values of the minimal conductivity for bilayer and single-layer of graphite are the same. In case of the bilayer, charges have energy spectrum drastically different from that for the single-layer case. The bilayer graphene is a zerogap semiconductor with parabolic touching of the electron and hole bands. The electrons here are no longer relativistic but preserve the chirality. In the next paper [27] Katsnelson calculated the minimal conductivity of graphene bilayer, using the Landauer formula, which gives $\sigma = \frac{e^2}{2h}$. The Fano factor for this system is $F = 1 - \frac{2}{\pi}$, which is rather close to the value 1/3 found for the single-layer case. As well as for the case of disordered metals. This means that the bilayer graphite is also characterized by some "intrinsic" disorder similar to the Zitterbewegung. To conclude, theories give the result for minimal conductivity value, $\sigma = \frac{e^2}{\pi h}$, (per valley per spin) for an ideal crystal.

In realistic crystals the conductivity is generically strongly affected by localization effects. One of the very general papers devoted to the study of electron transport properties of a disordered graphene is the paper of Ostrovsky *at el.* [29]. In particular authors consider influence of the disorder, which preserves chiral symmetry, on the value of minimal conductivity.

For calculations the Kubo formula was used

$$\sigma(\omega) = \frac{1}{2A}\int_0^{\infty} dt e^{i\omega t}\int_0^{\beta} d\lambda < j(t - i\lambda)\, j(0) >,$$

where $\beta = T^{-1}$ is the inverse temperature; A is the sample area and j is the current operator.

The linear dependence of the conductivity on the gate voltage that they found for the case of strong scattering agrees with the experimental findings [5,8], demonstrating that this kind of disorder is dominant in experimentally studied structures (Fig.3.2).

To determine the conductivity at the Dirac point, the case when disorder preserves one of the chiral symmetries of the Hamiltonian was analyzed. Some specific examples of chiral symmetry are (i) bond disorder due to distortions of the lattice, (ii) random magnetic field, (iii) dislocations, which are equivalent to a random non-Abelian gauge field, and (iv) infinitely strong short-range on-site impurities. For more detailed explanation of the symmetries of various types of disorders in graphene see Table 1 in Ref.[29]. The preservation of the chiral symmetry in the system gives the minimal conductivity of the order of e^2/h. The exact value still depends on the nature of a restriction on electron mean free path, which dependents on the physical setup (system size, dephasing length etc).

Whether disorder that preserves chiral symmetry is dominant in experimentally relevant structures remains an open question. Alternatively, a value of conductivity $\sim e^2/h$ at the Dirac point can emerge if the dominant disorder does not scatter electrons between two valleys [29]. Furthermore, macroscopic inhomogeneity (on the scale larger than the mean free path) is also important in measurements of $\sigma_{min.}$

Conclusions

To summarize, I presented a variety of quantum electrodynamical effects which can be observed in graphene.

Electrons in graphene are massless particles which effectively obey the relativistic Dirac equation with the Fermi velocity ~10^6 m/s instead of light speed. Such unique properties may be obtained from the well-known tight-binding model. The result of this model gives a conical intersection of valence and conduction bands at Brillouin zone edges. The existence of two equivalent Dirac points comes from the symmetry of the honeycomb lattice. Since the spectrum of fermions near intersection points is conical, fermions behave like massless particles obeying charge-conjugation symmetry.

The discovery of graphene offered a possibility of testing various QED effects, among which the "gedanken" Klein paradox and "Zitterbewgung" stand out because these effects are unobservable in particle physics. The effect of the Klein-like tunneling − unimpeded penetration of relativistic particles through extreme (high and wide) potential barriers − is well understood. Due to the zero band gap in graphene, there are always hole states aligned in energy and available inside the barrier (in the valence band) for the incoming electron. To achieve the overlap of electron and hole continuums in graphene the fields $\mathcal{E} \approx 10^5\,\mathrm{V\cdot cm^{-1}}$ (routinely accessible in experiments) should be sufficient, which is eleven orders of magnitude lower than what is necessary for the observation of the Klein paradox for elementary particles. This opens the possibility to test the Klein paradox in laboratory conditions using relatively small barriers (less then 1 eV). From another point of view, the Klein-like tunneling in graphene results in the charge carrier delocalization in the material, which potentially limits graphene applications. However, the Dirac quasiparticles can be confined by magnetic barriers.

Zitterbewegung − circular motion of elementary particles caused by an interference between positive and negative energy states − leads to the fluctuation of the position of an electron. This relativistic "jittering" of an electron in graphene could be interpreted in terms of classical physics as an interaction of electron with some potential caused by the presence of disorder in crystal. Therefore, the Zitterbewegung plays a role of "intrinsic" disorder in the system which appears in the presence of minimal conductivity of the ideal crystal (without scattering) even at zero temperatures.

Most theories suggest $\sigma_{\min} = 4e^2/h\pi$, which is about π times smaller than the typical values observed experimentally. The reason of disagreement is still an open question − "mystery of a missing pie". A value of conductivity $\sim e^2/h$ at the Dirac point can emerge in case of preservation of chiral symmetry by disorder or when the dominant disorder does not scatter electrons between two valleys. Furthermore, macroscopic inhomogeneity (on the scale larger than the mean free path) is also important for measurements of $\sigma_{\min}$.

Discovered only 4 years ago graphene is already one of the most studied carbon allotropes. But this material still poses a lot of theoretical and experimental questions, which have to be answered.

References:

1. A.K. Geim, K.S. Novoselov, The rise of graphene, Nature Materials, **6**, 183-191 (2007).
2. Nature Materials **6** (3), 169 (2007).
3. P.R. Wallace, The band theory of graphite, Phys. Rev. **71** (9), 622-634 (1947).
4. R. Saito, G. Dresselhaus, and M. S. Dresselhaus, Physical Properties of Carbon Nanotubes (Imperial, London, 1998).
5. K.S. Novoselov et al., Science **306**, 666 (2004).
6. S. Reich et al., Phys. Rev. B **66**, 035412 (2002).
7. G.W. Semenoff, Condensed-matter simulation of a three-dimensional anomaly, Phys. Rev. Lett. **53**, 2449-2452 (1984).
8. K.S. Novoselov et al., Two-dimensional gas of massless Dirac fermions in graphene, Nature **438**, 197-200 (2005).
9. M.I. Katsnelson, Graphene: carbon in two dimensions, Materials today **10** (1-2), 20-27 (2007).
10. F.D.M. Haldane, Model for a Quantum Hall Effect without Landau Levels: condenced-matter realization of the "parity anomaly", Phys. Rev. Lett. **61** (18), 2015-2018 (1988).
11. M.I. Katsnelson, Zitterbewegung, chirality, and minimal conductivity in graphene, Eur. Phys. J. B **51**, 157–160 (2006).
12. M. Wilson, Electrons in atomically thin carbon sheets behave like massless particles, Physics today, January, 21-23 (2006).
13. R. Jackiw, Fractional charge and zero modes for planar system in a magnetic field, Phys. Rev. D **29** (10), 2375-2377 (1984).
14. E. Fradkin, Critical behavior of disordered degenerate semiconductors. II. Spectrum and transport properties in mean-field theory, Phys. Rev. B **33** (5), 3263-3268 (1986).
15. R.L. Liboff, Introductory to quantum mechanics, Forth edition, Addison Wesley (San Francisco) 878 (2003).
16. A. Calogercos, N. Dombey, History and physics of Klein paradox, Contemporary Physics **40** (5), 313-321 (1999).
17. A. Calogercos, Paradox in a pencil, Nature Physics **2**, 579-580 (2006).
18. M.I. Katsnelson, K.S. Novoselov & A.K. Geim, Chiral tunneling and the Klein paradox in graphene, Nature Physics **2** (9), 620-625 (2006).
19. V.V. Cheianov, V. Fal'ko & B.L. Altshuler, Veselago lens electrons: focusing and caustics in graphene p-n junctions, arXiv:cond-mat/0703410v1 (2007).
20. M. Inman, Black hole in a pencil, ScienceNOW Daily News **3**, 23 August (2006).
21. Quoted by F. Bakke, H. Wergeland, Phys scripta **25**, 911 (1982).
22. A. De Martino et al., Magnetic confinement of massless Dirac fermions in graphene, Phys. Rev. Lett. **98**, 066802 (2007).
23. S. de Leo, Barrier paradox in the Klein zone, Phys. Rev. A **73**, 042107 (2006).
24. A.C. Neto et al., Drawing conclusions from graphene, Physics World, November (2006).

25. J. Cserti and G. David, Unified description of Zitterbewegung for spintronic, graphene, and superconducting systems, Phys. Rev. B **74**, 172305 (2006).
26. S.V. Morozov et al., Two-dimensional hole gases at the surface of graphite, Phys. Rev. B **72**, 201401(R), (2005).
27. M.I. Katsnelson, Minimal conductivity in bilayer graphene, Eur. Phys. J. B **52**, 151–153 (2006).
28. J. Tworzydlo et al., Sub-Poissonian shot noise in graphene, Phys. Rev. Let. **96**, 246802 (2006).
29. P.M. Ostrovsky, I.V. Gronyi, A.D. Mirlin, Electron transport in disordered graphene, Phys. Rev. B **74**, 235443 (2006).